Diffuse neutron scattering in sodium and potassium cyanide

J. M. Rowe
National Measurement Laboratory, National Bureau of Standards, Washington, D.C. 20234

S. Susman
Materials Science and Technology Division, Argonne National Laboratory, Argonne, Illinois 60439
(Received 27 October 1983)

Diffuse neutron scattering has been measured in NaCN at 295 K and KCN at 175 and 295 K. In both samples, strong scattering from the soft shear mode (related to the translation-rotation coupling which leads to the phase transition from the high-temperature cubic NaCl phase to the low-temperature orthorhombic phase) is observed. The asymmetry of this scattering about certain reciprocal-lattice points is direct evidence both of the bilinear nature of the coupling, and of its sign (and hence of the relative importance of overlap and quadrupolar interactions). In NaCN, additional structured diffuse scattering is observed which is absent in KCN at both measured temperatures. This scattering is assumed to arise from short-range order in CN orientations, but the data are not consistent with simple models of steric hindrance that have been proposed for the short-range correlations in NaCN.

INTRODUCTION

Sodium and potassium cyanide crystallize from the melt in the NaCl structure[1] with the $(CN)^-$ ions disordered[2,3] so as to achieve the requisite octahedral symmetry at the negative-ion site. As the temperature is lowered, two phase transitions occur[4]—first to a centered orthorhombic structure[5] in which the unique axis of the $(CN)^-$ ion orders but the sense of the ion does not (i.e., the electric quadrupole moment orders, but the electric dipole moment does not), and then to a primitive orthorhombic structure[6,7] in which the ions are fully ordered at 0 K. Haussühl[8,9] has shown that in the cubic phase, the elastic constant c_{44} in both KCN and NaCN has an anomalous temperature dependence, and this result has been explained[10,11] in terms of a bilinear coupling between the rotations of the $(CN)^-$ ions and the translational phonons.

The orientational distributions of the $(CN)^-$ ions in KCN and NaCN have been derived from single-crystal neutron-diffraction data[3] and confirmed by Raman scattering.[12] The surprising result of these measurements was that while in KCN the probability of finding a given C—N bond orientation was maximum in the [111] directions as would be expected from the ionic shapes and sizes, in NaCN the probability was maximum in the [100] directions. Coulon and Descamps[13] noted that this result was inconsistent with the known size of the Na^+ and $(CN)^-$ ions, and this implied that there must be strong short-range correlations in $(CN)^-$ orientations and Na^+ displacements. They calculated the x-ray diffuse scattering predicted from a simple model of steric hindrance and noted that the results were similar to the unpublished data of Levelut and Fontaine.[14] In order to further establish the existence and nature of short-range correlations in the alkali cyanides, the diffuse neutron scattering has been measured in KCN and NaCN. The theory of diffuse scattering is briefly reviewed in the next section, and the results of the current measurements are presented and discussed in the following two sections.

THEORY

The coherent neutron scattering cross section per atom for a system of N atoms can be written[15]

$$\frac{d^2\sigma}{d\omega\, d\Omega}=(k_f/k_i)(2\pi N)^{-1}\sum_{ij} b_i b_j \int \langle e^{-i\vec{Q}\cdot\vec{r}_i(0)} e^{i\vec{Q}\cdot\vec{r}_j(t)}\rangle e^{-i\omega t}dt\ , \tag{1}$$

where $\langle\ \rangle$ denotes a thermal average, $\hbar\omega$ equals energy transfer, $d\Omega$ is the unit of solid angle, k_f (k_i) is the scattered (incident) neutron wave vector, b_i is the coherent neutron scattering length, $\vec{r}_i(t)$ is the position of atom i at time t, and $\hbar\vec{Q}$ is the momentum transfer in the scattering process. In the present experiment the diffuse scattering was measured with an energy analyzer set for zero energy transfer, so that one measures essentially

$$\frac{d^2\sigma}{d\omega\, d\Omega}\Delta\omega = I(\Omega) \approx (2\pi N)^{-1}\sum_{ij} b_i b_j \int \langle e^{-i\vec{Q}\cdot\vec{r}_i(0)} e^{i\vec{Q}\cdot\vec{r}_j(t)}\rangle dt\ , \tag{2}$$

so that the measurements are sensitive only to those corre-

 ©1984 The American Physical Society

lations that are long-lived, i.e., those for which the decay time is long compared to $1/\Delta\omega$. In this case, one can replace Eq. (2) by

$$I(\Omega)=N^{-1}\left\{\sum_{ij} b_i b_j e^{-i\vec{Q}\cdot\vec{r}_i} e^{i\vec{Q}\cdot\vec{r}_j}\right\}, \tag{3}$$

where $\{\ \}$ indicates an average over long-lived configurations of the atoms in the crystal.

In the present case, where the atoms are combined into molecules, we can replace b_i by a molecular form factor

$$F_i=\sum_n b_n e^{-i\vec{Q}\cdot\vec{r}_n}, \tag{4}$$

where $\vec{r}_n$ is the position of the nth atom in the ith molecule. Substituting into Eq. (4), with an obvious generalization, we obtain

$$I(\Omega)=\left\{N^{-1}\sum_{ij} F_i F_j^* e^{i\vec{Q}\cdot\vec{r}_{ij}}\right\}. \tag{5}$$

Introducing a variable S_i to represent the orientation of a molecule at position r_i, and a joint probability $P(S_i,S_j)$ to represent the probability that the molecule at $\vec{r}_i$ has orientation S_i *and* that the molecule at $\vec{r}_j$ has orientation S_j, this equation can be rewritten as

$$\begin{aligned} I(\Omega)&=N^{-1}\sum_{S_i}\sum_{S_j}\sum_{i\neq j} P(S_i,S_j)F(S_i)F(S_j)^* e^{i\vec{Q}\cdot\vec{r}_{ij}}+\overline{F^2} \\ &=N^{-1}\sum_{S_i}\sum_{S_j}\sum_{i\neq j}[C(S_i,S_j)+P(S_i)P(S_j)] \\ &\quad\times F(S_i)F(S_j)e^{i\vec{Q}\cdot\vec{r}_{ij}}+\overline{F^2}, \end{aligned} \tag{6}$$

where

$$\overline{F^2}=\sum_{S_i} P(S_i)F(S_i)F(S_i)^*,$$

$$\bar{F}=\sum_{S_i} P(S_i)F(S_i),$$

$P(S_i)$ is the simple probability of finding an orientation S_i, and $C(S_i,S_j)=P(S_i,S_j)-P(S_i)P(S_j)$.

Then

$$I(\Omega)=I_B(\Omega)+C(\Omega)+D(\Omega), \tag{7}$$

where $I_B(\Omega)=N^{-1}\bar{F}^2\sum_{ij} e^{i\vec{Q}\cdot\vec{r}_{ij}}$, the Bragg scattering by the average crystal, $C(\Omega)=\overline{F^2}-\bar{F}^2$, the diffuse scattering in the absence of correlations, and

$$\begin{aligned} D(\Omega)=&-\bar{F}^2\sum_{n>1} e^{i\vec{Q}\cdot\vec{r}_{1n}} \\ &+\sum_{n>1}\sum_{S_1}\sum_{S_n} F(S_1)F(S_n)^*P(S_1,S_n)e^{i\vec{Q}\cdot\vec{r}_{1n}}. \end{aligned} \tag{8}$$

The last term, $D(\Omega)$, represents the diffuse scattering due to correlations in molecular orientations; this is the term of interest. This term has been discussed in detail[13] by Coulon and Descamps, who have given a method for developing this scattering in terms of the sum of a series of "weak graphs," and have applied the result to a particular model of steric hindrance in NaCN for x-ray scattering. Their calculation is readily adapted to the case of neutron scattering and we have done this. In their model the Na^+ ion is displaced along one of the cube edges [towards a $(CN)^-$ ion position], and the $(CN)^{-1}$ ion towards which it is displaced cannot be oriented along that axis. This model is claimed to be in at least qualitative agreement with the unpublished x-ray diffuse scattering results. In addition, we have developed a computer-simulation routine to calculate Eq. (8) directly, and we will compare the results of this model to the results.

EXPERIMENTAL RESULTS

The measurements were performed by using spectrometers at the National Bureau of Standards research reactor under many different experimental conditions in order to ensure that the effects seen are reproducible and representative of the sample. For most of the measurements shown below, the incident energy was fixed at 35.0 meV (wavelength $\lambda\approx 1.5$ Å), and the scattered beam was also energy analyzed (spectrometer set for zero energy transfer) by using the (002) planes of pyrolytic graphite with collimations of 30-25-25-42 minutes of arc before and after the monochromator and analyzer, respectively. In addition, several series of scans were done with the collimation increased to 20-12-12-20′, with an incident energy of 28.0 meV, and with no energy analyzer and collimations of 40-40-40-80′. For all of the measurements, a pyrolytic graphite filter 6 cm in length was used to suppress higher-order wavelengths from the monochromator.

For both NaCN and KCN, measurements were taken in the $(k_x\,k_y\,K_z)$ planes, with $K_z=0.0$, 0.5, 1.0, 1.5, and 2.0. The most pronounced structure was observed for $K_z=0.0$, and it is these results which will be shown. However, for NaCN, structured diffuse scattering was observed in all

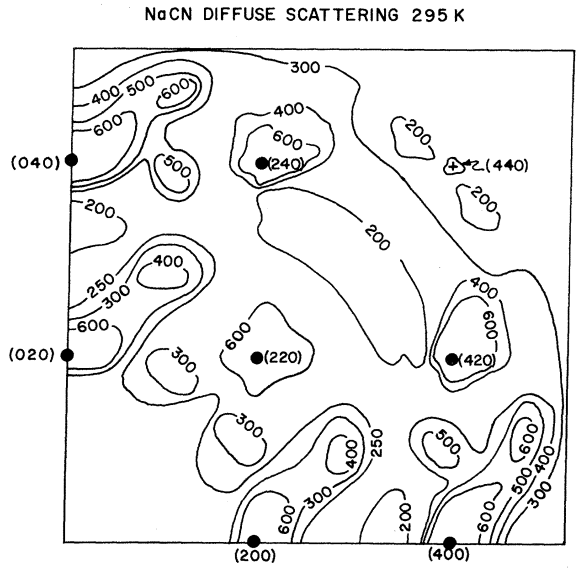

FIG. 1. Equal neutron-scattering-intensity contours in NaCN at 295 K in the (001) plane with energy analyzer in place. Reciprocal-lattice vectors given in units of $2\pi/a$.

planes measured. The results for NaCN at 295 K with $K_z=0.0$ are summarized in the contour plot in Fig. 1. Several features of the results shown in this figure should be noted.

(1) There is strong diffuse scattering centered at the Bragg points (200), (400), (220), and (420). This scattering is not isotropic in the plane for any Bragg point, and is asymmetric in the reduced wave vector $\vec{q}=(k_x,k_y,0)-(hk0)$; i.e., $I(\vec{q})\neq I(-\vec{q})$ near the (220) and (420) points.

(2) There are peaks in the diffuse scattering along $(k_x, 1.0, 0.0)$ with a period of approximately 1.0 in units of $2\pi/a$, where a is the cubic lattice parameter.

(3) There is a region with almost no scattering between (220) and (440).

(4) There is relatively little scattering at the (440) Bragg point.

In contrast to these results for NaCN, KCN shows almost no diffuse scattering at either 175 or 295 K *except* for that centered about Bragg points. This scattering is very similar to that found for NaCN, and the intensity increased dramatically as the temperature was lowered from 295 to 175 K (both samples are at $T/T_c\approx 1.04$, where T_c is the temperature at which the samples would undergo the phase transition to the orthorhombic structure). The relative absence of other diffuse scattering in KCN is shown in Fig. 2, where a scan along $(k_x, 1.0, 0.0)$ for KCN at 175 K is compared to the same cut for NaCN at 295 K.

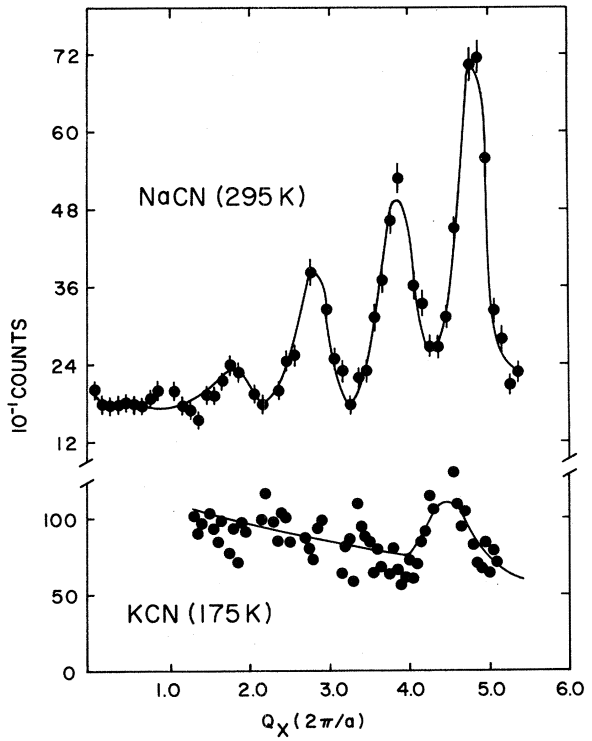

FIG. 2. Comparison of diffuse scattering along the line $(k_x, 1.0, 0.0)$ in NaCN at 295 K and KCN at 175 K. The counting times are equal, as are the sample volumes (note different scales). The solid lines are only a guide to the eye.

Although there appears to be some structure in the KCN sults, it is much smaller than that observed for NaCN.

Finally, in order to show the effects of using energy analysis on the diffuse scattering, Fig. 3 shows a comparison of a scan in NaCN along the $(k_x, 1.0, 0.0)$ direction with and without energy analysis. Clearly, the two scans show the same general structure, but the energy analysis suppresses the overall intensity (which increases as the wave vector increases) upon which the structure rides. Energy scans of the diffuse scattering in NaCN near the peaks along the $(k_x, 1.0, 0.0)$ direction show no energy broadening within the rather poor energy resolution ($\Delta E\approx 3$ meV). However, it is probable that all of the observed diffuse scattering is quasielastic, and that improved energy resolution would reveal the time scale of the correlations. It is impossible to increase the resolution significantly by using conventional techniques because of the momentum transfer required to observe the diffuse scattering.

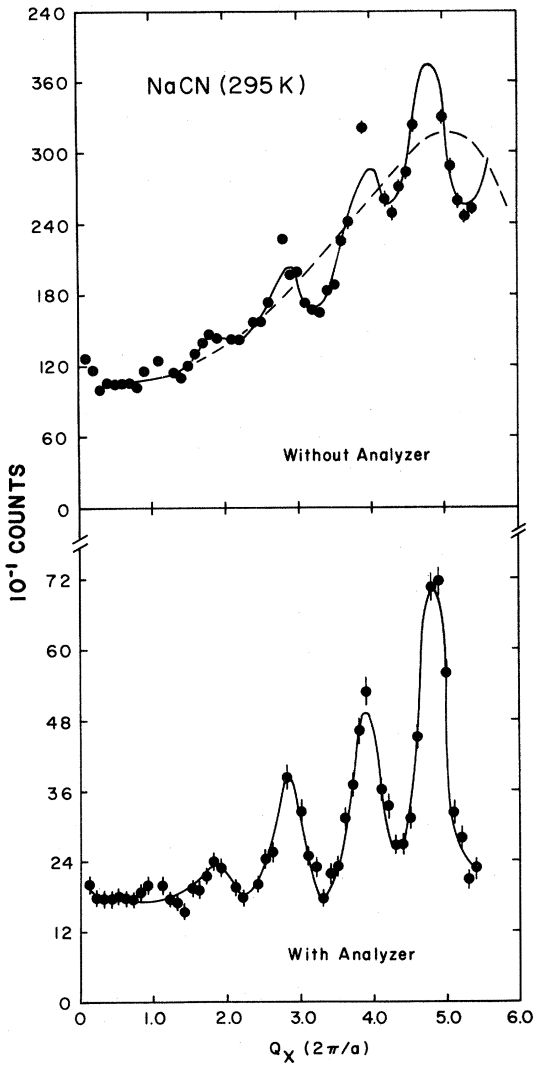

FIG. 3. Comparison of diffuse scattering in NaCN at 295 K with and without energy analyzer, for equal counting times. Solid lines are a guide to the eye, and dashed line in the upper curve is an estimate of the term $C(\Omega)$ (see text).

DISCUSSION

The results presented in the previous section can best be considered as two separate types of diffuse scattering, the first being that centered about Bragg points and the second being all other diffuse scattering. As pointed out in the Introduction, it is well known[8,9] that the c_{44} shear mode in both KCN and NaCN shows anomalous softening in the high-temperature cubic phase as the temperature is reduced towards the phase transition temperature. This shear constant determines the slope of the transverse acoustic modes propagating along the cube edges or [100] directions. (In fact, it determines the initial slope of all transverse acoustic modes propagating in planes perpendicular to the cube edges with polarization vectors perpendicular to the plane.) From neutron scattering measurements[16,17] it is known that the anomalous softening extends half way to the Brillouin zone boundary. The neutron scattering cross section for these modes has been derived by Michel and Naudts[18] in terms of a microscopic theory of translation-rotation coupling, including only repulsive Born-Mayer interactions in the potential of interaction between the K^+ and $(CN)^-$ ions. However, a subsequent molecular dynamics calculation[19] showed that anisotropic electrostatic forces [predominantly the quadrupole moment of the $(CN)^-$ ion interacting with the phonon displacements of the K^+ ions] were also important, and, in fact, were larger than the repulsive terms. This point was also elaborated in Ref. 11, which extended the static theory of Ref. 10 to include the electrostatic forces. In both Refs. 10 and 11, the softening of c_{44} (and thus the transverse acoustic branch) is shown to be the result of a bilinear coupling between translations and rotations. The rotational excitations are expressed in terms of correlation functions for fluctuations in symmetry-adapted spherical harmonics[20] of order $l=2$. For the octahedral symmetry of the $(CN)^-$ site, there are five such functions, two with E_g symmetry and three with T_{2g} symmetry. The functions of T_{2g} symmetry couple to c_{44} and are given by

$$\begin{aligned} Y_3&=(15/4\pi)^{1/2}xy\ , \\ Y_4&=(15/4\pi)^{1/2}zx\ , \\ Y_5&=(15/4\pi)^{1/2}yz\ , \\ x^2+y^2+z^2&=1\ . \end{aligned} \tag{9}$$

As shown in Ref. 18, the inelastic neutron scattering cross section is the sum of three terms, the first due to center-of-mass motions, the second to correlations of translations and rotations, and the third to rotations alone. For the case of a bilinear coupling, the second of these terms is odd in the reduced wave vector q, since it is the result of a correlation between a center-of-mass motion (a phonon, with scattering amplitude proportional to q) and a rotation (amplitude not proportional to q). The integrated intensity arising from this term can be shown to be proportional to $B=B_R+B_Q$, where B is the total translation-rotation coupling and B_R and B_Q are the repulsive and quadrupolar coupling terms, respectively. Since these two terms, B_R and B_Q, have opposite signs, the sign of B is determined by the relative magnitudes of the two contributions, and the sign of B can be determined directly from the contours in Fig. 1. Although the scattering from the translational-rotational (TR) coupling term is inelastic, with peaks at finite energy transfer, the energy resolution used is ($\Delta E\approx 3$ meV) such that the soft-mode intensity is included within the energy window (note from Ref. 16, that for $q=0.1$, $\omega\approx 0.4$ meV). Thus we can assign the intensity near the Bragg points to this scattering, and the symmetry about the (220) point is direct evidence of the bilinear nature of the coupling (this assignment has been checked by direct measurement of the energy dependence by using a resolution of 0.1 meV). As can be seen from Fig. 1, the intensity for $q>0.0$ is larger than for $q<0.0$ near the (220) reflection, and this implies that $|B_Q|>|B_R|$, as was suggested in Refs. 11 and 19. This is true for both KCN and NaCN, although only the results for NaCN are shown here. Thus the diffuse scattering near Bragg points is the result of inelastic processes (thermal diffuse scattering), and may be interpreted in terms of the TR coupling.

The absence of large scattering at the (440) Bragg point in NaCN is a result of the structure factor for Bragg scattering in the NaCl structure, along with the molecular form factor of the $(CN)^-$ ion. If one inserts the appropriate terms into Eq. (7), the structure factor governing the intensity of even-order Bragg reflections becomes

$$I_B \propto |b_{\mathrm{Na}}+\bar{F}|^2\ ,$$

where $\bar{F}$ is the molecular structure factor for the $(CN)^-$ ion at the Bragg point. An approximation to this structure factor is $b_{\mathrm{CN}}j_0(Qr_0)$, where $b_{\mathrm{CN}}=b_{\mathrm{C}}+b_{\mathrm{N}}$, $j_0(x)=\sin(x)/x$, and r_0 equals one half the C-N separation. The single-crystal diffraction results[3] show that this is a reasonable first-order approximation, and give $r_0\approx 0.6$ Å. Inserting the appropriate numbers, and noting that $Q(hkl)=(2\pi/a)(h^2+k^2+l^2)^{1/2}$, j_0 is negative at (440) and almost exactly cancels b_{Na} in the expression for the structure factor.

This leaves the second type of diffuse scattering in NaCN (that which is not centered at Bragg points) to be explained by correlations in $(CN)^-$ orientations as discussed in the theory section of this paper. We have compared our results with the predictions of a model similar to that proposed by Coulon and Descamps[13] based upon steric hindrance. The essential idea of this model can be seen from Figs. 4(a) and 4(b), where a reasonably accurate picture of the geometry in NaCN is shown. In (a) the lattice is shown with the $(CN)^-$ ions oriented along [100] directions and the Na^+ ions held at their symmetric positions (unrelaxed). As can be seen, this arrangement leads to substantial overlap of ionic cores, which can be relieved by the Na^+ displacements shown in (b). The net effect of this overlap and concomitant displacement is that second-neighbor $(CN)^-$ ions cannot both lie along the axis joining their centers of mass, an effect which leads to strong short-range order in their orientations. Rather than use the method of Ref. 13, we have simulated this arrangement on the computer, where it is easier to introduce other constraints. We have checked our program against the predictions of the method of Coulon and Descamps, and we find that the two methods agree provided that sufficient terms are included in the graph solutions. From

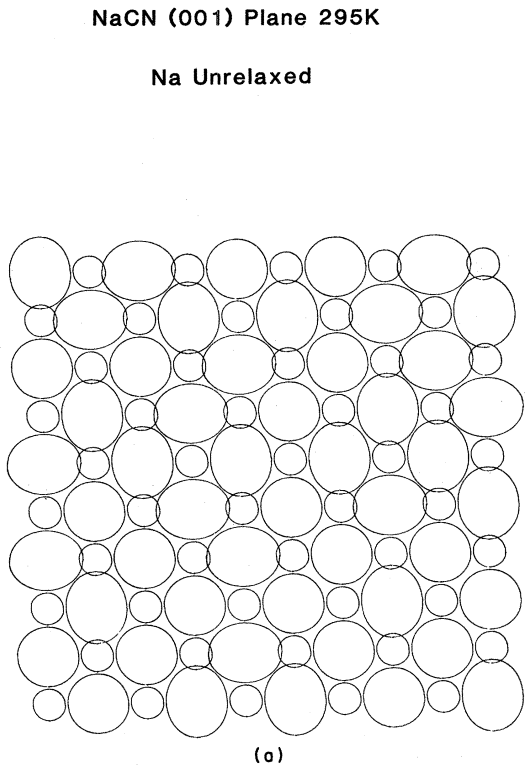

FIG. 4. Illustration of the approximate geometry of the NaCN structure, based on the ionic shape given in Ref. 5 and the lattice parameter $a = 5.87$ Å. (a) shows the situation when the Na^+ ions are constrained to remain at the lattice sites, while (b) shows the results of allowing a relaxation of the Na^+ ions to accommodate the nonspherical $(CN)^-$ ions. This effect is the basis of the model of steric hindrance given in Ref. 13 and discussed in the text.

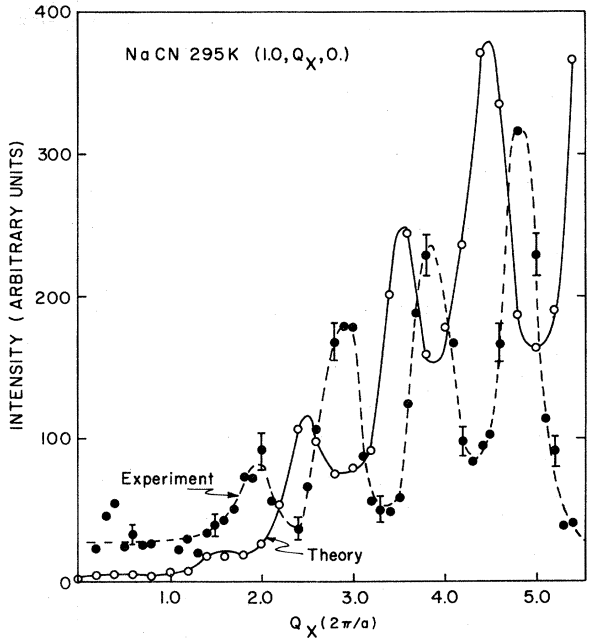

FIG. 5. Comparison of the predictions of the model of steric hindrance to the diffuse scattering in NaCN at 295 K, measured along the line $(1.0, q_x, 0.0)$. Note, that as discussed in the text, the theory includes the term $C(\Omega)$, while the measurements do not because of the energy analysis.

now on, we will refer exclusively to calculations done by the computer-simulation model when we discuss theoretical or model results. In Fig. 5 we show the results of a model calculation based upon the picture given in Fig. 4, compared to the measurements. In the model we have imposed the rule suggested by Fig. 4—namely, that two $(CN)^-$ ions separated by a distance a along one of the cubic axis directions cannot both point along the direction joining their centers of mass. We have constructed a computer model in which 500 $(CN)^-$ ions and 500 Na^+ ions are arranged on interpenetrating fcc lattices so that their centers of mass form a NaCl structure. We have also imposed periodic boundary conditions, so that the model is semi-infinite. The molecular orientations are chosen by starting from an arbitrary origin and assigning an orientation to the ion at this point by using a random number generator. The rest of the sites are filled by using both the rule stated above, and the random-number generator. The Na^+ ions are displaced from their nominal positions as shown in Fig. 2(b). When all sites are filled, the resultant configuration is used to construct a scattering function, either by calculating the probabilities $P(S_i, S_j)$ for use in Eq. (8), or by calculating the scattering directly from the definition in Eq. (3). A new configuration is then chosen in the same manner, the scattering is calculated and added to the first calculation, and the process is continued until the desired accuracy is achieved. The results shown in Fig. 5 were calculated by the direct method. However, they were also checked by calculating the probabilities P, and the two methods agreed well.

Note that the model contains the effects of the uncorrelated diffuse scattering $C(\Omega)$, so that the overall intensi-

ties increase as the wave vector increases. This uncorrelated scattering reflects the large rotational motion of the $(CN)^-$ ions, and is therefore distributed over a large energy range, as is shown by the results of Fig. 3, where the use of an energy analyzer with quite coarse resolution suppresses this scattering. The correlated scattering $D(\Omega)$, on the other hand, reflects the existence of relatively long-lived correlations of the $(CN)^-$ ions, and thus is distributed over a narrow energy range which falls entirely within the window of the analyzer. The use of a spectrometer with perfect energy resolution would suppress this scattering as well. The most striking feature of Fig. 5 is that the oscillations of the intensity are almost exactly out of phase. We have attempted to correct this failing by including the direct quadrupole-quadrupole interaction of the $(CN)^-$ ions in the calculations, with no improvement. We have also checked the calculations themselves by comparing them to the model calculation of Coulon and Descamps and by deriving simple limiting cases of the model assumed. We believe that the features of the curve shown, in particular the phase of the oscillations in intensity, arise from the central assumption of the model—namely, that second-neighbor $(CN)^-$ ions cannot both lie along the axis joining them. There is a further shortcoming of the model, in that it predicts that the scattering perpendicular to the scan direction shown extends further than along the scan direction, a result not in accord with the data (see Fig. 1).

We have been unable to derive a model that will explain the data completely, although the assumption that $(CN)^-$ ions prefer to align themselves along the axes joining second neighbors does change the phase of the oscillations to one closely resembling the data. In this case, however, the shape of the scattering is still too elongated along the direction perpendicular to the scan direction (k_x, 1.0, 0.0). In addition, we cannot find any physical reason for such an alignment of orientations. In fact, in the low-temperature monoclinic structure of RbCN and $(CN)^-$ ions do orient primarily along a cube edge in a long-range structure,[21] and the alignment is such that the model suggested by Fig. 4 would be appropriate. Thus we are unable to explain the data observed for NaCN by any simple model of steric hindrance, or, in fact, by any model whatsoever. Nonetheless, the scattering must be related to $(CN)^-$ correlations arising from the [100] average orientation fo the $(CN)^-$ ions, since it is absent in KCN, in which the ions are oriented primarily along [111] directions. We also know that the scattering arises from second-neighbor $(CN)^-$ ions, because of the period of the oscillations in intensity along the (k_x, 1.0, 0.0) direction, which also implies that steric hindrance is the source of the scattering. In spite of these considerations, we have been unable to construct a model structure that can explain the results.

ACKNOWLEDGMENTS

We acknowledge many useful discussions of this problem with our colleagues, in particular, E. Prince, J. Rush, M. Klein, and S. Werner.

[1]A. Cooper, Nature 107, 745 (1921); R. M. Bozorth, J. Am. Chem. Soc. 44, 317 (1922).
[2]D. L. Price, J. M. Rowe, J. J. Rush, E. Prince, D. G. Hinks, and S. Susman, J. Chem. Phys. 56, 3697 (1972).
[3]J. M. Rowe, D. G. Hinks, D. L. Price, S. Susman, and J. J. Rush, J. Chem. Phys. 58, 2039 (1973).
[4]E. Messer and W. T. Ziegler, J. Am. Chem. Soc. 63, 2610 (1941).
[5]H. J. Verweel and J. M. Bijvoet, Z. Kristallogr. 100, 201 (1938). J. M. Bijvoet and J. A. Lely, Rec. Trav. Chim. Pays-Bas Belg. 59, 908 (1940).
[6]D. Fontaine, C. R. Acad. Sci. Ser. B 281, 443 (1975).
[7]J. M. Rowe, J. J. Rush, and E. Prince, J. Chem. Phys. 66, 5147 (1977). J. M. Rowe, J. J. Rush, E. Prince, and N. J. Chesser, Ferroelectrics 16, 107 (1977).
[8]S. Haussühl, Solid State Commun. 13, 147 (1973).
[9]S. Haussühl, J. Eckstein, K. Recker, and F. Wallrafen, Acta Crystallogr. Sec. A 33, 847 (1977).
[10]K. H. Michel and J. Naudts, J. Chem. Phys. 67, 547 (1977).
[11]D. Sahu and S. D. Mahanti, Phys. Rev. B 26, 2981 (1982).
[12]D. Fontaine, R. Pick, and M. Yvinec, Solid State Commun. 21, 1095 (1977).
[13]G. Coulon and M. Descamps, J. Phys. C 13, 945 (1980).
[14]A. M. Levelut and D. Fontaine, private communication and Ref. 13.
[15]L. van Hove, Phys. Rev. 95, 249 (1954).
[16]J. M. Rowe, J. J. Rush, N. J. Chesser, K. H. Michel, and J. Naudts, Phys. Rev. Lett. 40, 455 (1978).
[17]J. M. Rowe, J. J. Rush, N. Vagelatos, D. L. Price, D. G. Hinks, and S. Susman, J. Chem. Phys. 62, 4551 (1975).
[18]K. H. Michel and J. Naudts, J. Chem. Phys. 68, 216 (1978).
[19]D. G. Bounds, M. L. Klein, and I. R. Macdonald, Phys. Rev. Lett. 46, 1682 (1981).
[20]See, for example, S. L. Altmann and A. P. Cracknell, Rev. Mod. Phys. 37, 19 (1965).
[21]J. M. Rowe, J. J. Rush, and F. Lüty, Phys. Rev. B 29, 2168 (1984).